Performance Evaluation of Contention-based Channel Access for mmWave Sidelink Communications

Alessandro Brighenti[#], Matteo Drago[*], Tommaso Zugno[*], Michele Zorzi[*], Paolo Casari[#]
[#]DISI, University of Trento, Italy. E-mail: alessandro.brighenti@studenti.unitn.it
[*]Department of Information Engineering, University of Padova, Italy. E-mail: {name.surname}@dei.unipd.it

***Abstract*—One of the main challenges of future automotive networks is the need to make vehicles aware of their surroundings. Each car will be required to collect data about the environment through dedicated sensors, and share it with its neighbors. Communicating in the millimeter wave spectrum could provide a solution for addressing such requirements. The huge amount of bandwidth available at millimeter wave frequencies, along with an optimized use of the physical resources, could provide massive data rates and low latency capabilities and enable the dissemination of real-time information. In this paper, we focus on platoons of vehicles that share LiDAR point-clouds with their platoon leader, and we use MilliCar, the ns-3 module based on the 3GPP NR V2X specifications, to provide an end-to-end performance evaluation. In particular, we study the trade-offs between using a semi-persistent resource allocation of time slots, with respect to a contention-based approach. By comparing different scheduling alternatives and different clear channel assessment thresholds, we show that coordination among different platoons can mitigate the inter-platoon interference and increase the reliability, whereas a contention-based approach achieves lower transmission delay.**

***Index Terms*—ns-3, mmWave, V2V, Millicar, sidelink, contention-based access**

I. Introduction

The regular use of a vehicle is one of the worst sources of air pollution. This is especially true in crowded scenarios such as traffic jams, where the typical human behavior is to repeatedly accelerate and brake. For this reason, in the past decades researchers have focused on solutions that could reduce the impact of the human factor, not only to limit pollution but also to save lives, the most ambitious being to make vehicles operate autonomously.

In this context, communications among different entities (cars, roadside infrastructure, remote sensors, etc.) is key to operating cooperative autonomous vehicle effectively. By communicating with each other, vehicles could easily agree whether to accelerate or brake based on road conditions, thus smoothing their drive and reducing emissions [1].

Since the initial release plan of 5th-generation (5G) networks, millimeter wave (mmWave) communications have been considered as one of the key technologies to enable extremely high data rates, in the order of multiple Gbps. Indeed, the mmWave spectrum between 30 and 300 GHz offers a large amount of available radio resources and enables very broadband communications [2]. Despite their potential, operating at mmWave frequencies presents several challenges related to the severe propagation losses that limit the communication range. To compensate for this effect, mmWave systems make use of large antenna arrays with beamforming capabilities, able to focus the transmit power towards the desired direction. While improving the channel gain and spatial diversity, this approach requires a coordination between source and destination about their relative position and antenna orientation [3].

In the last few years, mmWave communications are gaining attraction also for automotive applications, such as teleoperated driving, platooning, and HD map collecting and sharing. In particular, the high data rates achievable with mmWave devices makes it possible to share data generated by on-board sensors, like HD cameras or Laser Imaging Detection and Ranging (LiDAR) equipment [4], [5]. Depending on the configuration, each vehicle can generate Terabytes of data per hour [4]. Sharing this data with nearby vehicles is useful to improve their own perception of the surroundings, since a single vehicle could have a limited view, e.g., blocked by obstacles, buildings and other vehicles.

In this paper, we consider a platooning scenario where platoon members share sensor data with the leader through sidelink communications. We investigate the trade-off between scheduled and contention-based channel access schemes, and evaluate quantitatively whether the interference free transmissions allowed by scheduled schemes are worth the extra coordination and overhead required to set up the schedules. To this aim, we extend the functionalities of Millicar [6], a ns-3 module for the performance evaluation of novel solutions for Vehicle-to-Vehicle (V2V) networks.[1]

While in Section II and III we present channel access and related work in context of New Radio (NR) Vehicle-to-Everything (V2X), in Section IV we explain the implementation details of contention-based access in Millicar, in Section V we define the simulation scenario and, finally, in Section VI we present a thorough performance evaluation focusing on the measured mean Signal to Interference plus Noise Ratio (SINR), Packet Reception Ratio (PRR) and transmission delay. Also, we compare the results of the contention-based scheme against the scheduled approach in a scenario with two platoons of vehicles, for different parameters settings.

Tommaso Zugno was with University of Padova at the time the research was conducted and is now with Huawei Technologies, Munich Research Center.

This work received support from the European Commission's Horizon 2020 Framework Programme under the Marie Skłodowska-Curie Action MINTS (GA no. 861222).

[1]https://github.com/signetlabdei/mmwave-contention-based

II. Channel Access in NR V2X

As part of Rels. 16 and 17, the 3GPP introduced 5G NR V2X, a set of new functionalities for the 5G NR air interface to provide dedicated support to vehicular use cases [5]. This standard supports sidelink communications between User Equipments (UEs) and can operate at mmWave frequencies between 24.25 GHz and 71 GHz [7]. It enables the flexible configuration of physical layer parameters and slot formats to better adapt to different operating conditions, and supports two different modes for resource allocation and channel access. With Mode 1, UEs receive scheduling grants from the Next Generation NodeB (gNB) indicating which radio resources can be used for sidelink transmissions. This centralized management makes it possible to avoid collisions among transmissions from multiple vehicles, but requires UEs to be under the coverage of a gNB. With Mode 2, resource allocation is autonomously determined by each UE. In this case, as described in [8], the resource selection is performed at the Medium Access Control (MAC) layer, where a sensing-based procedure filters the slots that are used by other UEs. At slot n, candidate resources are examined and, eventually, some are potentially selected for transmission using Semi-Persistent Scheduling (SPS).

III. Related Work

Resource selection plays an important role for an efficient sharing of sidelink resources among vehicles in Mode 2 of 5G NR V2X. In [9], the authors present how the Modulation and Coding Scheme (MCS), Subcarrier Spacing (SCS) and the usage of blind retransmissions, affect the PRR and transmission range in Mode 2. Instead, in [10] the authors evaluate the impact of resource allocation policies on range and speed estimation in a highway scenario, taking into account the interference between vehicles. The work in [11] includes an algorithm to switch between cellular and sidelink mode to reduce traffic congestion and reduce the transmission delay in a highway scenario. There, vehicles are divided in clusters based on their position on the road.

Recently, several works in the literature have also proposed the use of Machine Learning (ML) techniques, and in particular of Reinforcement Learning (RL), to let devices agree upon transmission modes or channel access policies. RL provides a robust way to treat environment dynamics and their uncertainty [12]. For example, the authors of [13] use Multi-Agent Reinforcement Learning (MARL) to learn a channel access policy and its signaling strategies in multiple-access Uplink (UL) scenarios, i.e., where a Base Station (BS) receives data sent from a group of UEs. This framework, in particular, can produce application-tailored protocols that outperform the throughput of contention-based solutions, when the required data rate is high. In [14], instead, RL is used to adaptively select different transmission control policies based on the current network status in Software-Defined Vehicular Networking (SDVN), with the objective of improving throughput. In fact, in this type of scenarios, the performance of different transmission control schemes varies according to network conditions. Finally, Zhao *et al.* propose to select the communication mode and the power level through an RL agent, with the objective of guaranteeing Quality of Service (QoS), high capacity of Vehicle-to-Infrastructure (V2I) links and reliability of V2V links [12]. Each connection among the vehicles is modeled as an RL agent that makes decisions based on the surrounding environment, such as the interference from V2V and V2I transmitters.

In our work, we consider a scenario where vehicles communicate through their sidelink interface operating in the mmWave band. In this context, we evaluate the performance of a contention-based channel access scheme and compare it against a semi-persistent scheduled approach. In the next section, we detail the implementation of our contention-based approach.

IV. Contention-based Channel Access in Millicar

MilliCar is an ns-3-based simulation tool for the end-to-end evaluation of V2V communications at mmWave frequencies [6]. The channel model is based on the 3GPP TR 38.901 specifications and its extensions for vehicular propagation environment modeling [15]. MilliCar devices implement a sidelink protocol stack compliant with the 3rd Generation Partnership Project (3GPP) specifications. At the physical and MAC layers, Millicar implements a Time Division Duplexing (TDD)-based frame structure, where each timeframe of 10 ms is divided into 10 subframes of 1 ms each. Each subframe is further divided into a variable number of slots (each composed of 14 Orthogonal Frequency Division Multiplexing (OFDM) symbols), that depends on the selected *numerology*. As of now, the module supports NR numerologies 2 and 3, corresponding to a SCS of 60 kHz and 120 kHz, respectively. While numerology 2 divides the subframe in 4 slots of 0.250 ms each, for numerology 3 there are 8 slots of 0.125 ms each.

By default, Millicar supports a coordination policy between the sender and the receiver of the communication: this consists of a semi-persistent Time Division Multiple Access (TDMA)-based channel access scheme, in which a fixed number of slots is assigned to each vehicle through a pre-configured scheduling policy. Specifically, time slots are distributed among devices based on the communication group they belong to. In this way, at the start of each slot, a device is configured to send data (if it has something to transmit), and another to receive. All the others remain idle, and they can only access the channel during their predefined slots. As a consequence, considering that the current version of the module does not feature any round-robin policy, if we use numerology 3 we can support up to a maximum of 8 non-interfering users per simulation, each assigned to a distinct time slot. Note that, however, vehicles associated to different communication groups can also transmit during the same time slot, possibly leading to packet collision and interference. Also, in this case the slots of a subframe can be equally divided among the number of users. For example, if each communication group has four vehicles, each device will be assigned two slots. Further details about this mechanism will be provided in Section V.

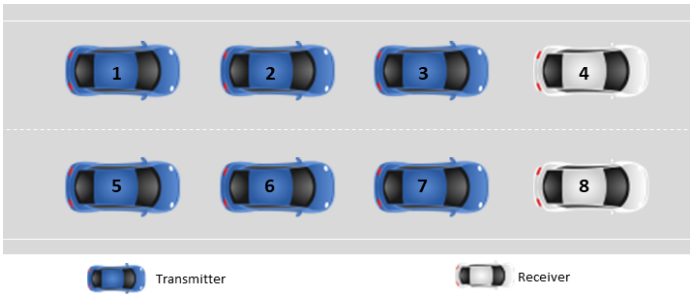

Fig. 1. Simulation scenario.

The above semi-persistent scheduling scheme has the advantage of assigning orthogonal communication resources to users in the same group, thus preventing collisions. However, it requires strict coordination among group members, since they need to agree on a common communication schedule. Moreover, it does not prevent collisions among devices belonging to different groups and/or with other systems operating at the same frequency, such as radars.

Through the design of a contention-based solution, we eliminate the need of the semi-persistent scheme, thus removing its limitations as well. With this approach, every device can send data as soon as it senses an idle communication channel, i.e., there is no instantaneous interference. We remark that we consider every received signal that was directed to some other node as interference.

With respect to the code structure, in Millicar the class `MmWaveSidelinkSpectrumPhy` handles the transmission and reception operations at the physical layer. In this class we implemented a new method to declare the channel as idle when the sensed interference is under a threshold value θ, specified as a parameter at the start of simulation. The class `MmWave-SidelinkMac`, instead, implements MAC layer functionalities and distributes the available resources, i.e., decides which device has transmit/receive in a particular slot.

`MmWaveSidelinkMac` was modified to include our new contention-based channel access, as an alternative to the default scheduled-based scheme previously supported by MilliCar. In particular, in the new version of the code the status of the channel is checked after the beginning of each slot to make sure that transmitting devices already started their transmissions. Then, if the channel is idle, the device can transmit for the entire slot duration. After that, before a subsequent transmission the state of the channel has to be validated again. If, instead, the channel is busy, the device has to wait for a random number of slots, uniformly distributed between 0 and 8 (i.e., between 0 ms and 1 ms), before checking again if it can transmit. We set the upper bound of number of slots in the backoff window to 8, so that the waiting time is at most equal to the duration of a subframe.

V. Simulation scenario

In our simulation scenario, (Fig. 1) we mimic a highway environment by configuring two platoons of four vehicles each, traveling in the same direction. Each platoon member moves at a constant speed s of 20 m/s, and the distance between other platoon members is $d_{inter} = 15\ m$.

TABLE I
Simulation parameters

Parameter	Description	Value
f_c	Frequency	28 GHz
B	Bandwidth	100 MHz
P_{TX}	Transmission power	30 dBm
F_p	LiDAR frame period	50 ms
MCS	Modulation and coding scheme	28
s	Speed of vehicles	20 m/s
t	Simulation time	11 s
d_{intra}	Intra-group distance	{20, 40, 80} m
d_{inter}	Inter-group distance	15 m
A_{elem}	Number of antenna elements	{1, 4, 16}
θ	Interference threshold	{−330, −290, −200, −160, −120} dBW/Hz
R_{TX}	Transmission data rate	{1.42, 15.99, 21.34} Mbps
O_{res}	Orthogonal resources on different groups	{True, False}

Within a platoon, the leader acts as the receiver, while all the other devices transmit sensor data. To enable mmWave sidelink directional communication, vehicles are equipped with a 4×4 phased antenna array, and configured so that platoon members directs their highest-gain beam towards the leader.

From the point of view of the higher layers, each transmitter is equipped with the uplink application streaming LiDAR data [16], modeled according to the Kitti multi-modal dataset [17]. The different values of transmission data rate R_{TX} that we will consider in the following are derived from and empirical study of the dataset. Receivers are set up with a sink to only receive data. The LiDAR frame period F_p is set to 50 ms, in line with common LiDAR characteristics [18], [19].

We performed some preliminary tests by setting the distance between vehicles of the same platoon (d_{intra}) to 20 m and 40 m. This allowed us to measure the interference sensed by each device. As a result, we defined −120 dBW/Hz, as a "non-sensing" threshold θ, i.e., a device will always consider the channel as idle and try to transmit, raising the probability of collisions. Conversely, we chose −330 dBW/Hz as the lowest value of θ. This is equivalent to trying to transmit if and only if there is zero interference on the channel, thus minimizing the probability of collisions among concurrent transmissions.

As described in Section IV, coordinating the communicating vehicles is fundamental when using a scheduled channel access policy, as we need to define beforehand how many slots are allocated to each device in every subframe. Moreover, we can define communication groups so that devices within the same group are assigned orthogonal slots. In our evaluation, we considered two different cases: (i) all the vehicles in the scenario belong to the same communication group ($O_{res} =$ `True`), and (ii) each platoon corresponds to a different communication group ($O_{res} =$ `False`).

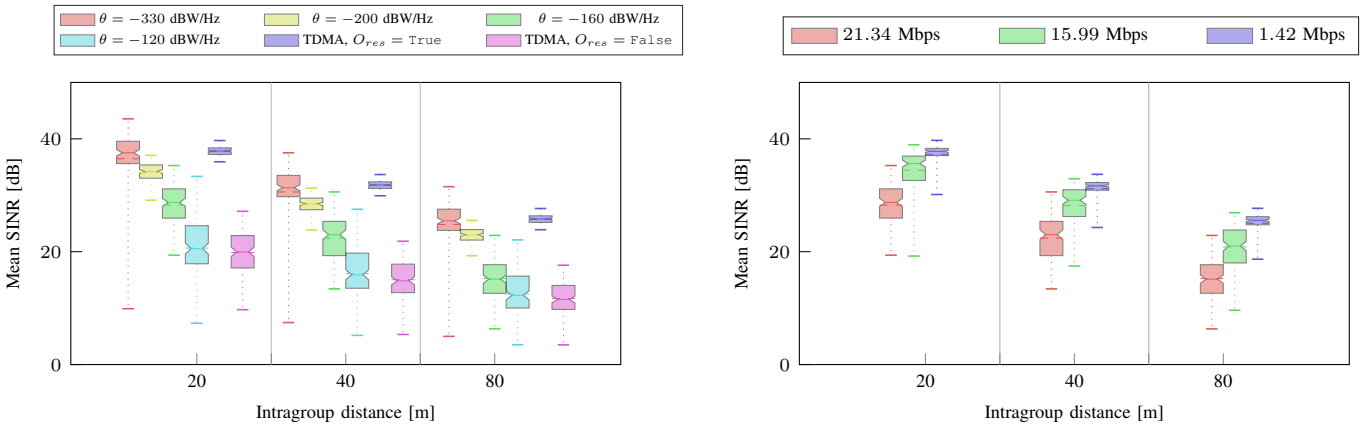

(a) Schemes comparison for $R_{TX} = 21.34$ Mbps.

(b) Contention-based scheme with $\theta = -160$ dBW/Hz.

Fig. 2. Mean SINR obtained for $A_{elem} = 4$.

On the contrary, in a contention-based architecture, there is no need to preemptively declare the transmission schedule, thus removing the need for coordination and limiting the signaling overhead. In this case, the parameter θ is fundamental to define the amount of interference that can be tolerated without causing collisions. A comprehensive list of simulation parameters can be found in Table I.

VI. Results

For our study we tested how different values of θ affect the SINR, PRR (evaluated as the ratio between the number of packets received by the sink application at the receiver and the number of packets transmitted by the uplink application) and the end-to-end transmission delay. We compared all results with those of MIlliCar's default scheduled-based approach.

Specifically, in each of the presented figures, we use box and whiskers plots, where the edges of the box represent the 25th and 75th percentiles (first and third quartiles), the line in the middle of each box is the median, the notches of the boxes are the 95% Confidence Interval (CI) around the median, the dotted line is the mean of the represented quantity and, finally, the whiskers identify outliers.

For each metric we present two complementary plots: in the first one we fix $A_{elem} = 4$ and $R_{TX} = 21.34$ Mbps, comparing different channel access policies. In the second one, instead, we fix $\theta = -160$ dBW/Hz, analyzing the results for different values of R_{TX}.

A. SINR

The SINR represents the strength of the received signal with respect to the interference and noise. The higher the SINR, the better the signal quality. In Fig. 2a, we evaluate the distribution of the SINR across different executions by varying d_{intra}. We observe that the TDMA-based scheme achieves the best SINR thanks to coordination of transmissions among devices of different groups (O_{res} = `True`). This is always the case, even for different values of d_{intra}. If we look at the interquartile range (IQR), the contention-based policy's threshold that guarantees the closest results is $\theta = -330$ dBW/Hz, that corresponds to the case when a device transmit only when there is no interference.

On the other hand, when $\theta = -120$ dBW/Hz, i.e., the "non-sensing" threshold, the SINR is in general the lowest among all policies, as we transmit even if we sense interference. Also, in this case the lower outliers of the boxplot have the smallest values with respect to every other scheme, while the central part of the distribution is equivalent to the TDMA-based case with O_{res} = `False`. Although the two schemes achieve comparable results, the contention-based policy does not require the overhead of sharing a transmission schedule among all the members of the platoon. An intermediate threshold, $\theta = -160$ dBW/Hz, shows balanced results (between $\theta = -330$ dBW/Hz and $\theta = -120$ dBW/Hz), in particular in the IQR and when $d_{intra} = 20$ m.

Fig. 2b shows the distribution of the SINR with different R_{TX} and d_{intra}. We observe that the SINR is higher for lower values of R_{TX}, in particular for the IQR of the distribution. This is expected, as with a lower number of transmitted packets we have a smaller collision probability, which limits interference and increases the average SINR.

B. PRR

Next, we analyze the distribution of the PRR for different values of d_{intra} and different channel access policies in Fig. 3a.

First, we notice that the majority of IQRs of the contention-based approach with $\theta = -200$ dBW/Hz outperforms the scheduled-based scheme with O_{res} = `True`. This confirms that this value of θ leads to very few collisions and that low thresholds yield a mean PRR above 0.6 even with $d_{intra} = 80$ m (i.e., the farthest transmitting devices are at 240 m from the respective receivers).

Moreover we observe that the contention-based scheme with $\theta = -330$ dBW/Hz leads to unstable results: the IQR covers almost all the whiskers space, in particular with $d_{intra} =$

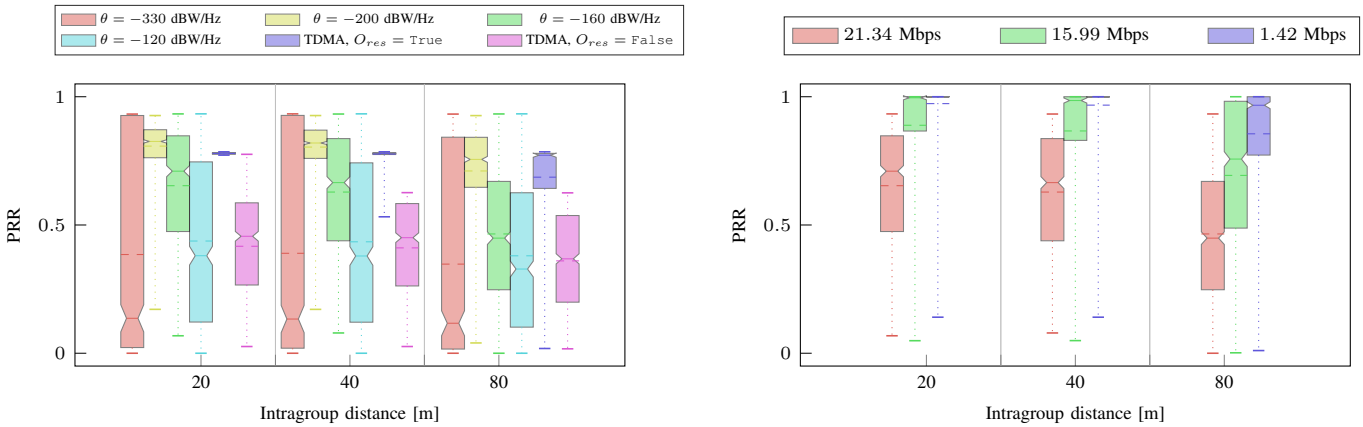

(a) Schemes comparison for $R_{TX} = 21.34$ Mbps.

(b) Contention-based scheme with $\theta = -160$ dBW/Hz.

Fig. 3. Mean PRR obtained for $A_{elem} = 4$.

$\{20, 40\}$ m. Also, the mean value of PRR is the worst among all the different access policies. With $R_{TX} = 21.34$ Mbps, the application generates so many packets that the transmission buffer of the application is filled up before they can be sent, because of the very low θ. Thus, packets are discarded and flagged as "not transmitted." Having a full buffer leads to a PRR always less than 1, even considering the outliers of the distribution, for every channel access policy.

As pointed out above, with $\theta = -120$ dBW/Hz it is more likely to have collisions and, consequently, packet losses. This is confirmed by the IQR, that is very large and completely below the one associated to $\theta = -200$ dBW/Hz.

In Fig. 3b, we plot the PRR for different values of R_{TX} and d_{intra}. First, we can notice that R_{TX} has a huge influence on PRR: in general, the higher the data rate, the lower the PRR. This trend is observed especially for a low d_{intra}, where the IQR of $R_{TX} = 21.34$ Mbps is all below the one of $R_{TX} = 15.99$ Mbps, while for $d_{intra} = 80$ m we confirm a higher variability, even with a low R_{TX}, due to the fact that all devices are farther from the receiver. Notably, with more transmitted packets, it is easier to experience collisions between packets, especially with high values of θ, which allow a node to transmit even if the channel is crowded. With $R_{TX} = 1.42$ Mbps, and $d_{intra} = \{20, 40\}$ m, collisions rarely occur, hence the PRR is very likely equal to 1.

C. Delay

In Fig. 4 we plot the Empirical Cumulative Distribution Function (ECDF) of the trasmission delay for each channel access policy with $d_{intra} = \{20, 40\}$ m. We can immediately notice that contention-based policies experience lower delay than TDMA-based schemes. With semi-persistent schemes, in fact, every device can transmit in 1 (with $O_{res} = \texttt{True}$) or 2 (with $O_{res} = \texttt{False}$) slots per subframe, deteriorating the overall performance, especially if the application generates data at a fast pace. Moreover, when a device seizes the channel, all the packets waiting in the MAC queue are sent back-to-back. Only above 2 ms of measured latency do we observe that the policy using $\theta = -200$ dBW/Hz is outperformed by TDMA with $O_{res} = \texttt{False}$. This, however, could be caused by packets that wait longer in tramission queues if they find the channel busy. In general, with a contention-based approach, packets wait less time in queue, since they are sent as soon as the channel is declared idle. In addition, with a non-sensing θ packets are dispatched irrespective of the channel state, and they are sent as soon as they arrive at the MAC layer, resulting in the lowest experienced delay. By looking at the SINR, delay and PRR jointly, we can obtain a more complete picture of the performance of scheduled and contention-based medium access. For example, for $\theta = -120$ dBW/Hz contention-based access achieves the lowest end-to-end delay, but also the highest packet loss. In fact, the threshold is so high that we transmit even in case of heavy interference. While guaranteeing immediate access to the channel, this also leads to a higher probability of collisions. This has to be taken into account when setting the parameters of the chosen MAC scheme.

Finally, in Fig. 5 we show the ECDF of transmitting delay for different values of R_{TX} and we further confirm that, the higher the application data rate, the higher the experienced delay, since more packets will most likely end up waiting in the transmission queue, based on the implemented policy. In fact, with the smallest data rate ($1.42\,\mathrm{Mbps}$) the distribution of the delay is mostly under $1\,\mathrm{ms}$.

VII. Conclusions

In this paper, we proposed an end-to-end performance evaluation that focuses on the trade-offs between different resource scheduling strategies, in a mmWave communication scenario. In particular, we compare the performance in terms of SINR, PRR and delay of a contention-based scheme with respect to a TDMA-based semi-persistent scheduling approach. We performed our simulations using the MilliCar ns-3 module, in a scenario with 8 vehicles divided in two platoons, where each platoon member shares LiDAR data with its leader.

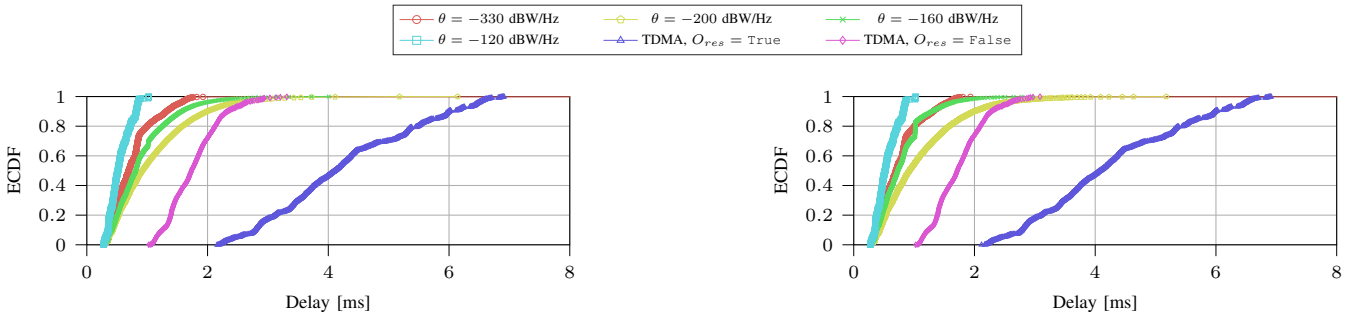

(a) Intragroup distance 20 m.

(b) Intragroup distance 80 m.

Fig. 4. Delay ECDF obtained for $A_{elem} = 4$ and fixed $R_{TX} = 21.34$ Mbps.

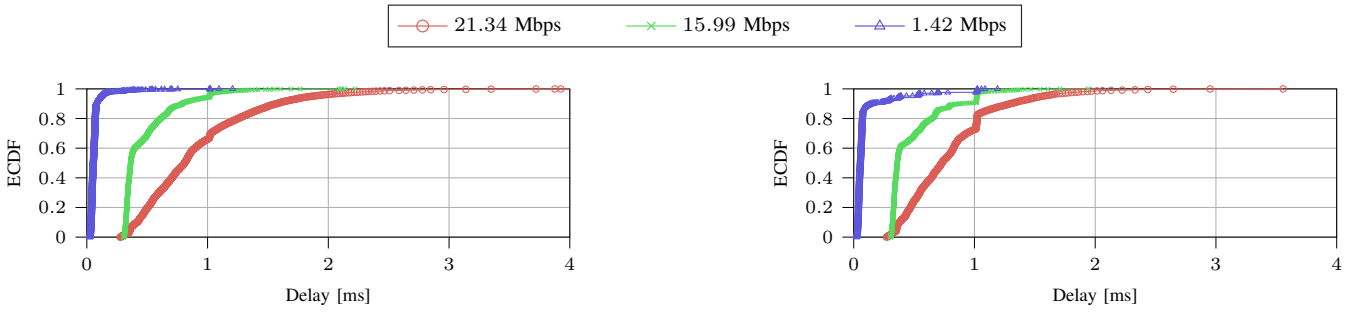

(a) Intragroup distance 20 m.

(b) Intragroup distance 80 m.

Fig. 5. Delay ECDF obtained for $A_{elem} = 4$ and fixed $\theta = -160$ dBW/Hz.

Results highlighted that contention-based schemes shows a remarkable improvement in terms of delay with respect to a scheduled approach, with a slight deterioration of SINR depending on the interference threshold. To conclude, while TDMA can provide a higher degree of control to the designer, contention-based schemes are suitable under stricter latency constraints, at the expense of a lower PRR.

Future extensions of this work include the evaluation of more challenging scenarios with a higher number of vehicles following more sophisticated trajectories, and with different parameter settings. Also, the scheduler could be integrated with additional features to account for other aspects of the 3GPP standardization process.

REFERENCES

[1] J. Gonder *et al.*, "Analyzing vehicle fuel saving opportunities through intelligent driver feedback," National Renewable Energy Lab. (NREL), Golden, CO (United States), Tech. Rep., 2012.

[2] S. Rangan *et al.*, "Millimeter-wave cellular wireless networks: Potentials and challenges," *Proc. of the IEEE*, vol. 102, no. 3, Mar. 2014.

[3] M. Giordani *et al.*, "A Tutorial on Beam Management for 3GPP NR at mmWave Frequencies," *IEEE Commun. Surveys Tuts.*, vol. 21, no. 1, pp. 173–196, 2019.

[4] J. Choi *et al.*, "Millimeter-wave vehicular communication to support massive automotive sensing," *IEEE Commun. Mag.*, vol. 54, no. 12, pp. 160–167, Dec. 2016.

[5] T. Zugno *et al.*, "Toward standardization of millimeter-wave vehicle-to-vehicle networks: Open challenges and performance evaluation," *IEEE Commun. Mag.*, vol. 58, no. 9, pp. 79–85, Sep. 2020.

[6] M. Drago *et al.*, "MilliCar: An ns-3 module for mmWave NR V2X networks," in *Proc. WNS3*, Gaithersburg, MD, USA, Jun. 2020.

[7] 3GPP, "NR; User Equipment (UE) radio transmission and reception; Part 2: Range 2 Standalone," TR 38.101-2 V17.6.0, Jun. 2022.

[8] Z. Ali *et al.*, "3GPP NR V2X Mode 2: overview, models and system-level evaluation," *IEEE Access*, 2021.

[9] V. Todisco *et al.*, "Performance analysis of sidelink 5G-V2X mode 2 through an open-source simulator," *IEEE Access*, vol. 9, pp. 145 648–145 661, 2021.

[10] S. Bartoletti *et al.*, "Sidelink 5G-V2X for integrated sensing and communication: the impact of resource allocation," in *Proc. IEEE ICC Workshops*, 2022, pp. 79–84.

[11] H. D. R. Albonda and J. Pérez-Romero, "An efficient mode selection for improving resource utilization in sidelink V2X cellular networks," in *Proc. IEEE CAMAD*. IEEE, 2018, pp. 1–6.

[12] D. Zhao *et al.*, "A reinforcement learning method for joint mode selection and power adaptation in the V2V communication network in 5G," *IEEE Trans. on Cogn. Commun. and Netw.*, vol. 6, no. 2, pp. 452–463, 2020.

[13] M. P. Mota *et al.*, "Scalable joint learning of wireless multiple-access policies and their signaling," *arXiv preprint arXiv:2206.03844*, 2022.

[14] M. Liu *et al.*, "Deep reinforcement learning based adaptive transmission control in vehicular networks," in *2021 IEEE 94th Veh. Technol. Conf. (VTC2021-Fall)*. IEEE, 2021, pp. 1–5.

[15] T. Zugno *et al.*, "Extending the ns-3 spatial channel model for vehicular scenarios," in *Proc. of the 2021 Workshop on Ns-3*, 2021.

[16] M. Lecci *et al.*, "An ns-3 implementation of a bursty traffic framework for virtual reality sources," in *Proc. WNS3*, 2021, pp. 73–80.

[17] A. Geiger *et al.*, "Are we ready for autonomous driving? the kitti vision benchmark suite," in *Conf. on Comp. Vision and Pattern Recognit. (CVPR)*, 2012.

[18] I. Maksymova *et al.*, "Review of LiDAR sensor data acquisition and compression for automotive applications," *MDPI Proceedings*, vol. 2, no. 13, pp. 1–4, 2018.

[19] X. T. Nguyen *et al.*, "A high-definition LIDAR system based on two-mirror deflection scanners," *IEEE Sensors J.*, vol. 18, no. 2, pp. 559–568, 2017.